

Electrochemical and Analytical Study on 3-Carbohydrazide Derivatives as Corrosion Inhibitors for Different Types of Low C-Steel in Acidic Medium

Hala M. Hassan^{*1}, A. M. Eldesoky², A. Attia³ and Awad Al-Rashdi⁴

¹Textile Technology Department, Industrial Education College, Beni-Suef University, Egypt and Chemistry Department, Faculty of Science, Jazan University, KSA. E-mail: dr.halamahfooz@yahoo.com

²Engineering Chemistry Department, High Institute of Engineering & Technology (New Damietta), Egypt and Al-Qunfudah Center for Scientific Research (QCSR), Al-Qunfudah University College, Umm Al-Qura University, KSA.

³Department of Chemistry, Faculty of Science, Mansoura University, Mansoura, Egypt and Faculty of Science and Arts in Balgarn, Chemistry Department, Bisha University, KSA.

⁴Al-Qunfudah Center for Scientific Research (QCSR), Chemistry Department, Al-Qunfudah University College, Umm Al-Qura University, KSA.

Abstract— Three 3-carbohydrazide derivatives have been investigated for the corrosion of different types of low C-steel in 2 M HCl solution at different concentrations at $25 \pm 1^\circ\text{C}$ using potentiodynamic polarization, electrochemical impedance spectroscopy (EIS) and electrochemical frequency modulation (EFM) techniques. Generally, inhibition efficiency of the investigated compounds was found to depend on the concentration and the nature of the inhibitors. These studies have shown that 3-carbohydrazide derivatives are very good “green”, mixed-type inhibitors. Electrochemical frequency modulation (EFM) and electrochemical impedance spectroscopy (EIS) method of analysis are also presented here for monitoring corrosion. Corrosion rates obtained from both EFM and EIS methods are comparable with those recorded using Tafel extrapolation method, confirming validation of corrosion rates measured by the latter. The inhibitive action of these 3-carbohydrazide derivatives was discussed in terms of blocking the electrode surface by adsorption of the molecules through the active centers contained in their structures. Quantum chemical method was also employed to explore the relationship between the inhibitor molecular properties and its protection efficiency. The density function theory (DFT) is used to study the structural properties of 3-carbohydrazide derivatives. The protection efficiencies of these compounds showed a certain relationship to highest occupied molecular orbital (HOMO) energy, Mulliken atomic charges and Fukui indices. The corrosion resistance of alloyed low C-steel surface layer with 1% Cu type (B) was better than alloyed low C-steel surface layer with 0.5 % Cu type (A).

Index Terms— Low C-steel, HCl, EFM, EIS, Fukui Indices.

1 INTRODUCTION

Acid solutions are widely used in industry, such as acid pickling of iron and steel, chemical cleaning and processing, ore production and oil well acidification [1–3]. The problems arising from acid corrosion required the development of various corrosion control techniques among which the application of chemical inhibitors has been acknowledged as most economical method for preventing acid corrosion [4–9]. Many organics, such as quaternary ammonium salts, acetylenic alcohol, and heterocyclic compounds are widely used as inhibitors in various industries. The organic molecules adsorb on the metal surface through heteroatom, such as nitrogen, oxygen and sulfur, blocking the active sites and generating a physical barrier to reduce the transport of corrosive species to

the metal surface [10–16]. Other researches revealed that the adsorption is influenced not only by the nature and surface charge of the metal, but also by the chemical structure of inhibitors. Among these organic compounds, heterocyclic substances containing nitrogen atoms, such as 4-aminoantipyrine compounds are considered to be excellent corrosion inhibitors in combating acidic corrosion due to high inhibition efficiency, good thermal stability and lack of irritating odor for many metals and alloys in various aggressive media [17–22]. Therefore, the develop of novel modified inhibitors containing 4-aminoantipyrine heterocyclic ring and the study of the relations between the chemical structure of inhibitors and their inhibition performances are of great importance, both from the

industrial and theoretical points of view.

This paper aims at investigating of the inhibition effect and electrochemical behavior of 3-carbohydrazide derivatives for different types of low C-steel in 2 M HCl solution by the potentiodynamic polarization, electrochemical impedance spectroscopy (EIS) and electrochemical frequency modulation (EFM) techniques. Several quantum-chemistry calculations have been performed in order to relate the inhibition efficiency to the molecular properties of the different types of compounds [23–25]. The aim of this study also was to obtain low C-steel alloying with Cu by powder metallurgy (PM) cladding and to investigate the corrosion performance of the alloy thus obtained.

2. EXPERIMENTAL DETAIL

2.1. Composition of Material Samples

TABLE 1

CHEMICAL COMPOSITION (WT%) OF DIFFERENT TYPES OF C-STEEL

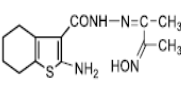
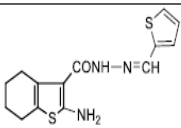
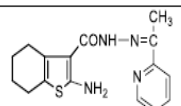
Type	C	Mn	P	Si	Cu	Fe
A	0.200	0.350	0.024	0.003	0.5	rest
B	0.200	0.350	0.024	0.003	1.0	rest

2.2. Chemicals and Solutions

Hydrochloric acid (37 %), ethyl alcohol and acetone were purchased from Al-gomhoria Company. Bidistilled water was used throughout all the experiments.

TABLE 2

MOLECULAR STRUCTURES, FORMULAS AND MOLECULAR WEIGHTS OF THE INVESTIGATED 3-CARBOHYDRAZIDE DERIVATIVES [26].

Comp.	Structure	Name	Chemical formula	M.Wt
(I)		amino-N-(3-(hydroxyimino)butan-2-ylidene)-4,5,6,7-tetrahydrobenzo [b]thiophene-3-carbohydrazide	$C_{13}H_{16}N_4O_3S$	294.37
(II)		amino-N-(thiophen-2-ylmethylene)-4,5,6,7-tetrahydrobenzo [b]thiophene-3-carbohydrazide	$C_{14}H_{14}N_4O_2S_2$	305.42
(III)		amino-N-(1-(pyridin-2-yl) ethylidene)-4,5,6,7-tetrahydrobenzo [b]thiophene-3-carbohydrazide	$C_{16}H_{14}N_4OS$	341.41

mostated three electrode cell. Platinum foil was used as counter electrode and a saturated calomel electrode (SCE) coupled to a fine Luggin capillary as the reference electrode. The working electrode was in the form of a square cut from different types of low C-steel under investigation and was embedded in a Teflon rod with an exposed area of 1 cm². This electrode was immersed in 100 ml of a test solution for 30 min until a steady state open-circuit potential (E_{ocp}) was attained. Potentiodynamic polarization was conducted in an electrochemical system (Gamry framework instruments version 3.20) which comprises a PCI/ 300 potentiostat, controlled by a computer recorded and stored the data. The potentiodynamic curves were recorded by changing the electrode potential from -1.0 to 0.0 V versus SCE with scan rate of 5 mV/s. All experiments were carried out in freshly prepared solution at constant temperature (25 ±1 °C) using a thermostat. IE% and the degree of surface coverage (θ) were defined as:

$$\% IE = \theta \times 100 = [(i_{corr} - i_{corr(inh)})/i_{corr}] \times 100 \quad (1)$$

Where i_{corr} and $i_{corr(inh)}$ are the uninhibited and inhibited corrosion current density values, respectively, determined by extrapolation of Tafel lines.

The electrochemical impedance spectroscopy (EIS) spectra were recorded at open circuit potential (OCP) after immersion the electrode for 15 min in the test solution. The ac signal was 5 mV peak to peak and the frequency range studied was between 100 kHz and 0.2 Hz. All Electrochemical impedance experiments were carried out using Potentiostat/Galvanostat/ Zra analyzer (Gamry PCI 300/4). A personal computer with EIS300 software and Echem Analyst 5.21 was used for data fitting and calculating.

The inhibition efficiency (%IE) and the surface coverage (θ) of the used inhibitors obtained from the impedance measurements were calculated by applying the following relations:

$$\% IE = \theta \times 100 = [1 - (R_{ct}/R_{ct})] \quad (2)$$

Where, R_{oct} and R_{ct} are the charge transfer resistance in the absence and presence of inhibitor, respectively.

EFM experiments were performed with applying potential perturbation signal with amplitude 10 mV with two sine waves of 2 and 5 Hz. The choice for the frequencies of 2 and 5Hz was based on three arguments [27]. The larger peaks were used to calculate the corrosion current density (i_{corr}), the Tafel slopes (β_c and β_a) and the causality factors CF-2 and CF-3 [28]. All electrochemical experiments were carried out using Gamry instrument PCI300/4 Potentiostat/Galvanostat/Zra analyzer, DC105 Corrosion software, EIS300 Electrochemical Impedance Spectroscopy software, EFM140 Electrochemical Frequency Modulation software and Echem Analyst 5.5 for results plotting, graphing, data fitting and calculating.

2. 4. Theoretical Study

Accelrys (Material Studio Version 4.4) software for quantum chemical calculations has been used.

3. RESULTS AND DISCUSSION

3.1. Potentiodynamic Polarization Measurements

Figs (1, 2) show the potentiodynamic polarization curves for different types of low C-steel without and with different concentrations of compound (I). Similar curves for other compounds were obtained and are not shown at 25 °C. The obtained electrochemical parameters; cathodic (β_c) and anodic (β_a) Tafel slopes, corrosion potential (E_{corr}), and corrosion current density (i_{corr}), were obtained and listed in Tables (3,4). Tables (3,4) shows that i_{corr} decreases by adding the 3-carbohydrazide compounds and by increasing their concentration. In addition, E_{corr} does not change obviously. Also β_a and β_c do not change markedly, which indicates that the mechanism of the corrosion reaction of different types of low C-steel does not change. Figs. (1,2) clearly shows that both anodic and cathodic reactions are inhibited, which indicates that investigated compounds act as mixed-type inhibitors [29-30]. The inhibition achieved by these compounds decreases in the following order: Compound(III) > Compound(II) > Compound(I).

Also, the results of θ and % IE where calculated using i_{corr} values. The percentage inhibition efficiencies (%IE) calculated from i_{corr} of the investigated compounds is given in Tables (3, 4). An inspection of the results obtained from this Table reveals that, the presence of different concentrations of the additives reduces the anodic and cathodic current densities and the polarization resistance. This indicates that the inhibiting effects of the investigated compounds. The order of decreasing inhibition efficiency from i_{corr} is: Compound(III) > Compound(II) > Compound(I).

TABLE 3

THE EFFECT OF CONCENTRATION OF THE INVESTIGATED COMPOUNDS ON THE FREE CORROSION POTENTIAL (E_{corr}), CORROSION CURRENT DENSITY (i_{corr}), TAFEL SLOPES (β_a & β_c), INHIBITION EFFICIENCY (% IE), AND DEGREE OF SURFACE COVERAGE FOR THE CORROSION OF LOW C-STEEL TYPE (A) IN 2 M HCL AT 25°C.

Compound	Conc.,M.	$-E_{corr}$,Mv (vs SCE)	i_{corr} , $\mu A cm^{-2}$	β_a , $mV dec^{-1}$	β_c , $mV dec^{-1}$	θ	% IE
(I)	Blank	434	2.24	48	122	----	----
	5×10^{-6}	475	1.99	81	139	0.111	11.1
	7×10^{-6}	474	1.95	88	133	0.129	12.9
	9×10^{-6}	448	1.84	60	159	0.178	17.8
	11×10^{-6}	455	1.80	64	135	0.196	19.6
	13×10^{-6}	474	1.79	82	125	0.201	20.08
	15×10^{-6}	448	1.78	59	155	0.205	20.5
(II)	5×10^{-6}	491	1.56	127	181	0.304	30.4
	7×10^{-6}	487	1.50	88	126	0.330	33.0
	9×10^{-6}	482	1.48	85	135	0.339	33.9
	11×10^{-6}	487	1.46	86	124	0.348	34.8
	13×10^{-6}	460	1.41	63	138	0.371	37.1
	15×10^{-6}	472	1.34	94	21.	0.402	40.2
(III)	5×10^{-6}	482	1.31	79	125	0.415	41.5
	7×10^{-6}	460	1.30	59	131	0.419	41.9
	9×10^{-6}	491	1.29	105	156	0.424	42.4
	11×10^{-6}	476	1.17	87	163	0.478	47.8
	13×10^{-6}	487	1.12	102	155	0.500	50.0
	15×10^{-6}	494	1.06	113	152	0.527	52.7

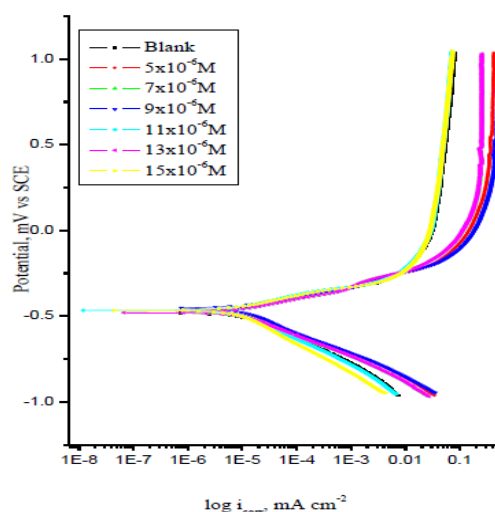
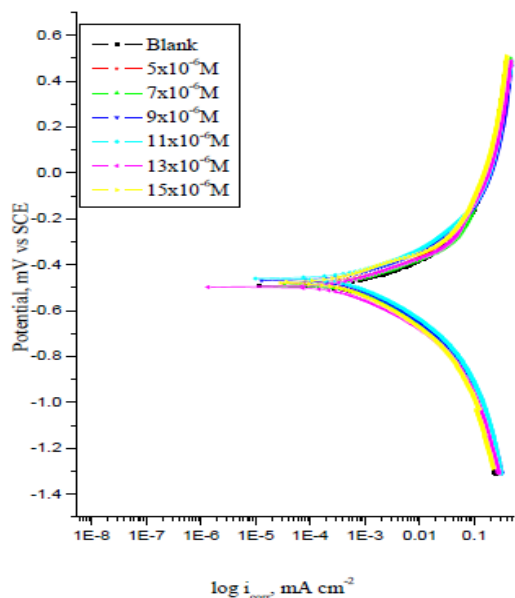


Fig. 1: Potentiodynamic Polarization Curves for the Corrosion of Low C-Steel Type (A) in 2 M HCl in the Absence and Presence of Various Concentrations of Compound (I) at 25°C.

Fig. 2: Potentiodynamic Polarization Curves for the Corrosion of Low C-Steel Type (B) in 2M HCl in the Absence and Presence of Various Concentrations of Compound (I) at 25°C.

TABLE 4

THE EFFECT OF CONCENTRATION OF THE INVESTIGATED COMPOUNDS ON THE FREE CORROSION POTENTIAL (E_{CORR}), CORROSION CURRENT DENSITY (i_{CORR}), TAFEL SLOPES (BA & BC), INHIBITION EFFICIENCY (% IE), AND DEGREE OF SURFACE COVERAGE FOR THE CORROSION OF LOW C-STEEL TYPE (B) IN 2M HCL AT 25°C.

Compound	Conc., M	E_{CORR} , mV(vs SCE)	i_{CORR} , $\mu A\ cm^{-2}$	β_a , mV dec ⁻¹	β_c , mV dec ⁻¹	θ	% IE
(I)	Blank	494	6.00	81	126.8	----	-----
	5×10^{-6}	481	4.80	78	123.7	0.200	20.0
	7×10^{-6}	489	4.48	77	109	0.253	25.3
	9×10^{-6}	467	4.04	81	118	0.326	32.6
	11×10^{-6}	459	3.55	77	106	0.408	40.8
	13×10^{-6}	497	3.073	82	111	0.487	48.7
	15×10^{-6}	477	3.04	95	114	0.493	49.3
(II)	5×10^{-6}	492	2.97	85	120	0.505	50.5
	7×10^{-6}	472	2.79	79	101	0.535	53.5
	9×10^{-6}	492	2.06	85	120	0.656	65.6
	11×10^{-6}	472	2.01	79	101	0.665	66.5
	13×10^{-6}	448	1.87	70	114	0.688	68.8
	15×10^{-6}	483	1.82	69	107	0.696	69.6
(III)	5×10^{-6}	472	1.80	41	66	0.700	70.0
	7×10^{-6}	463	1.75	36	46	0.708	70.8
	9×10^{-6}	486	1.75	65	96	0.713	71.3
	11×10^{-6}	487	1.61	81	97	0.781	73.1
	13×10^{-6}	491	1.57	82	106	0.738	73.8
	15×10^{-6}	460	1.48	97	121	0.753	75.3

The corrosion of different types of low C-steel in 2 M HCl in the presence of the investigated compounds was investigated by EIS method at 25 °C after 30 min immersion. Nyquist plots in the absence and presence of investigated compound (1) is presented in Figs (3, 4). Similar curves were obtained for other inhibitors. It is apparent that all Nyquist plots show a single capacitive loop, both in uninhibited and inhibited solutions. The impedance data of different types of low C-steel in 2M HCl are analyzed in terms of an equivalent circuit model Fig. (5) which includes the solution resistance R_s and the double layer capacitance C_{dl} which is placed in parallel to the charge transfer resistance R_{ct} [31] due to the charge transfer reaction. For the Nyquist plots it is obvious that low frequency data are on the right side of the plot and higher frequency data are on the left. This is true for EIS data where impedance usually falls as frequency rises (this is not true for all circuits). The capacity of double layer (C_{dl}) can be calculated from the following equation:

$$C_{dl} = \frac{1}{2\pi f_{max} R_{ct}} \quad (3)$$

Where f is the maximum frequency at which the imaginary part (Zimg) of the impedance is a maximum. The parameters obtained from impedance measurements are given in Tables (5, 6). It can be seen from Table (5, 6) that the values of charge transfer resistance R_{ct} increase with inhibitor concentration [32]. In the case of impedance

studies, %IE increases with inhibitor concentration in the presence of investigated inhibitors and the % IE of these investigated inhibitors is as follows:

Compound (III) > Compound(II) > Compound(I).

The impedance study confirms the inhibiting characters of these compounds obtained from potentiodynamic polarization. It is also noted that the (C_{dl}) values tend to decrease when the concentration of these compounds increases. This decrease in (C_{dl}), which can result from a decrease in local dielectric constant and/or an increase in the thickness of the electrical double layer, suggests that these compounds molecules function by adsorption at the metal/solution interface [33]. The inhibiting effect of these compounds can be attributed to their parallel adsorption at the metal solution interface. The parallel adsorption is owing to the presence of one or more active center for adsorption.

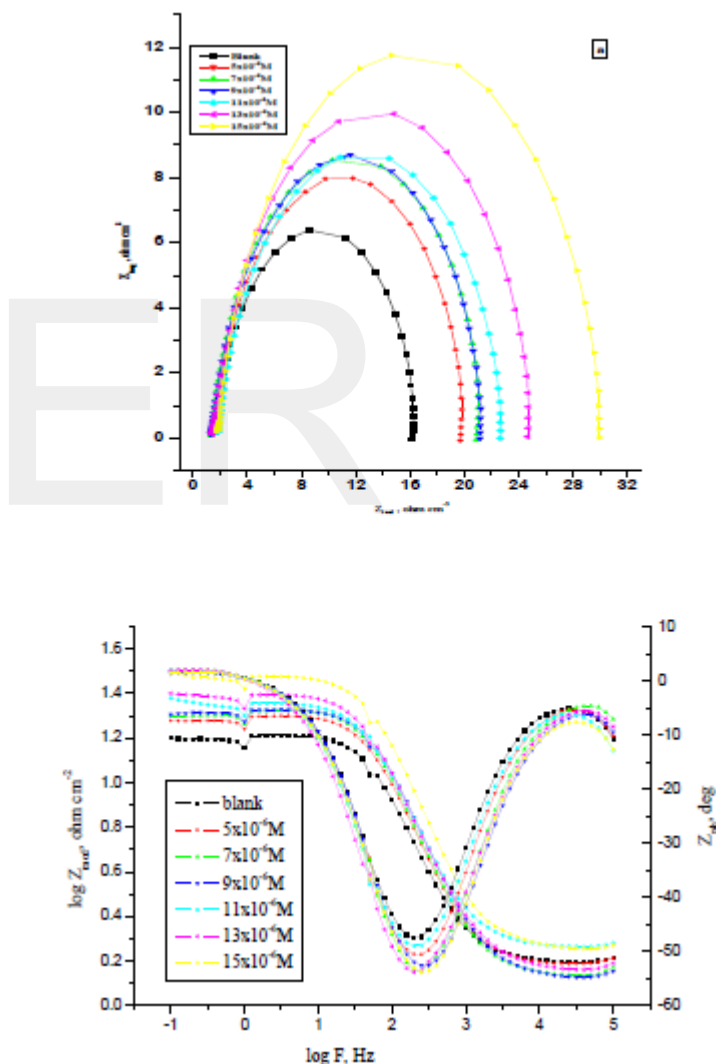


Fig. 3: The Nyquist (a) and Bode (b) Plots for Corrosion of Low C-steel Type (A) in 2 M HCl in the Absence and Presence of Various Concentrations of Compound (I) at 25°C.

TABLE 5

ELECTROCHEMICAL KINETIC PARAMETERS OBTAINED BY EIS TECHNIQUE FOR LOW C-STEEL TYPE (A) IN 2 M HCL WITHOUT AND WITH VARIOUS CONCENTRATIONS OF COMPOUNDS (I-III) AT 25 °C.

Compound	Conc.,M	R_s , Ωcm^2	$Y_o \times 10^{-3}$, $\mu\Omega^{-1}\text{s}^n$	n	R_{ct} , Ωcm^2	C_{dl} , $\times 10^{-3}$, μFcm^{-2}	θ	%IE
(I)	Blank	11.81	134.1	804.9	1.013	99.32	-----	-----
	5×10^{-6}	11.08	160.6	763.6	1.256	80.17	0.193	19.3
	7×10^{-6}	1.115	52.24	849.7	1.373	73.20	0.262	26.2
	9×10^{-6}	9.882	87.94	759.6	1.453	69.26	0.303	30.3
	11×10^{-6}	14.12	178.1	737.3	1.492	67.53	0.321	32.1
	13×10^{-6}	9.92	154.8	764.7	1.581	63.70	0.359	35.9
	15×10^{-6}	10.35	81.57	796.5	1.636	61.50	0.381	38.1
	17×10^{-6}	2.635	85.72	804.4	1.679	59.92	0.397	39.7
(II)	5×10^{-6}	9.966	90.12	802.7	1.693	59.43	0.402	40.2
	7×10^{-6}	9.886	163.6	767.2	1.737	57.99	0.415	41.5
	9×10^{-6}	1.361	39.83	858.2	1.777	56.55	0.429	42.9
	11×10^{-6}	10.16	110.2	803.1	1.778	56.63	0.430	43.0
	13×10^{-6}	1.348	37.28	845.0	1.779	56.49	0.431	43.1
	15×10^{-6}	9.449	123.4	794.8	1.824	55.19	0.445	44.5
	17×10^{-6}	9.510	148.7	807.7	1.895	53.14	0.465	46.5
	19×10^{-6}	1.477	33.22	845.8	2.068	48.59	0.510	51.1
(III)	5×10^{-6}	1.672	33.01	832.7	2.256	44.55	0.551	55.1
	7×10^{-6}	1.624	30.59	826.5	2.808	35.80	0.639	63.9
	9×10^{-6}	11.99	289.8	1.580	6.872	17.824	0.853	85.3
	11×10^{-6}							
	13×10^{-6}							
	15×10^{-6}							
	17×10^{-6}							
	19×10^{-6}							

TABLE 6

ELECTROCHEMICAL KINETIC PARAMETERS OBTAINED BY EIS TECHNIQUE FOR LOW C-STEEL TYPE (B) 2 M HCL WITHOUT AND WITH VARIOUS CONCENTRATIONS OF COMPOUNDS (I-III) AT 25 °C.

Compound	Conc.,M	R_s , Ωcm^2	$Y_o \times 10^{-3}$, $\mu\Omega^{-1}\text{s}^n$	n	R_{ct} , Ωcm^2	C_{dl} , μFcm^{-2}	θ	%IE
(I)	Blank	1.570	352.1	878.2	40.40	69.68	-----	-----
	5×10^{-6}	1.54	284.2	892.5	17.97	56.18	0.194	19.4
	7×10^{-6}	1.38	262.0	895.0	19.29	52.336	0.249	24.9
	9×10^{-6}	1.346	266.5	878.0	19.72	51.207	0.265	26.5
	11×10^{-6}	1.830	301.9	872.1	20.91	48.306	0.307	30.7
	13×10^{-6}	1.458	303.1	866.3	23.34	43.28	0.379	37.9
	15×10^{-6}	1.791	211.0	875.7	28.42	35.91	0.485	48.5
	17×10^{-6}							
(II)	5×10^{-6}	1.344	389.8	880.5	28.48	35.48	0.491	49.1
	7×10^{-6}	1.519	357.0	889.6	28.91	34.95	0.499	49.9
	9×10^{-6}	1.499	246.3	901.1	32.42	3.117	0.553	55.3
	11×10^{-6}	1.474	279.3	900.6	40.87	24.72	0.645	64.5
	13×10^{-6}	1.776	400.0	866.7	42.2	23.96	0.657	65.7
	15×10^{-6}	1.543	208.0	888.0	50.45	20.029	0.713	71.3
	17×10^{-6}							
	19×10^{-6}							
(III)	5×10^{-6}	1.275	341.8	887.5	51.36	19.689	0.718	71.8
	7×10^{-6}	1.566	219.5	898.9	50.08	17.39	0.751	75.1
	9×10^{-6}	1.500	303.1	897.5	60.33	16.75	0.759	75.9
	11×10^{-6}	1.817	398.1	851.7	60.96	16.59	0.762	76.2
	13×10^{-6}	2.211	260.4	885.5	85.73	11.74	0.831	83.1
	15×10^{-6}	2.452	112.0	868.3	267.6	37.81	0.946	94.6
	17×10^{-6}							
	19×10^{-6}							

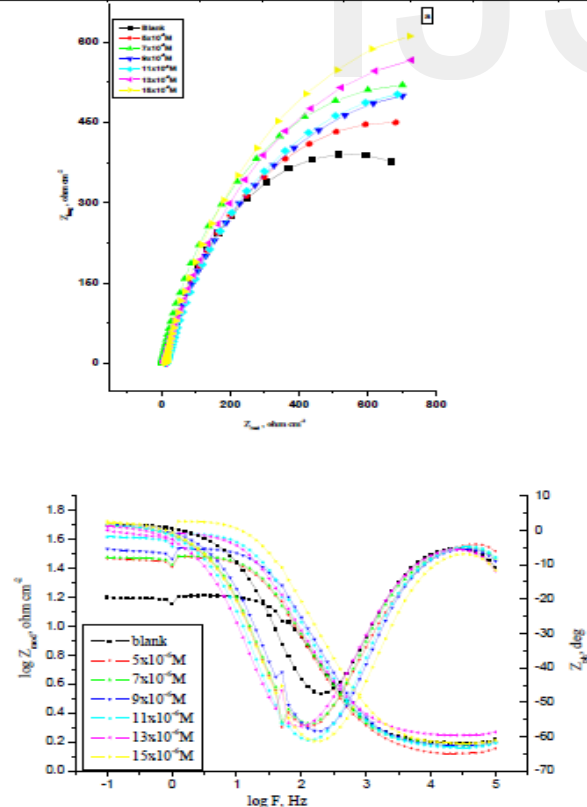


Fig. 4: The Nyquist (a) and Bode (b) Plots for Corrosion of Low C-steel Type (A) in 2 M HCl in the Absence and Presence of Various Concentrations of Compound (I) at 25°C.

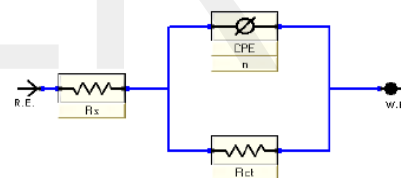


Fig. 5: Equivalent Circuit Model Used to Fit the Impedance Spectra

3.3. Electrochemical Frequency Modulation Technique (EFM)

EFM is a nondestructive corrosion measurement technique that can directly and quickly determine the corrosion current value without prior knowledge of Tafel slopes, and with only a small polarizing signal. These advantages of EFM technique make it an ideal candidate for online corrosion monitoring [34]. The great strength of the EFM is the causality factors which serve as an internal check on the validity of EFM measurement. The causality factors CF-2 and CF-3 are calculated from the frequency spectrum of the current responses. Figs (6, 7) shows the frequency spectrum of the current response of different types of low C-steel in 2 M HCl, contains not only the input frequencies, but also contains frequency components which are the sum, difference, and multiples of the two input frequencies. The EFM intermodulation spectrums of different types of low C-steel in 2 M HCl acid solution containing (5×10^{-6} - 15×10^{-6} M) of the studied inhibitors are shown in Figs (6, 7). Similar results were recorded for the other concentrations of the investigated compound (not shown). The harmonic and intermodulation peaks are clearly visible and are much larger than the background noise. The two large peaks, with amplitude of about 200

μA , are the response to the 40 and 100 mHz (2 and 5 Hz) excitation frequencies. It is important to note that between the peaks there is nearly no current response ($<100 \text{ nA}$). The experimental EFM data were treated using two different models: complete diffusion control of the cathodic reaction and the "activation" model. For the latter, a set of three non-linear equations had been solved, assuming that the corrosion potential does not change due to the polarization of the working electrode [35]. The larger peaks were used to calculate the corrosion current density (i_{corr}), the Tafel slopes (β_c and β_a) and the causality factors (CF-2 and CF-3). These electrochemical parameters were simultaneously determined by Gamry EFM140 software, and listed in Tables (7, 8). The data presented in Tables (7, 8) obviously show that, the addition of any one of tested compounds at a given concentration to the acidic solution decreases the corrosion current density, indicating that these compounds inhibit the corrosion of different types of low C-steel in 2 M HCl through adsorption. The causality factors obtained under different experimental conditions are approximately equal to the theoretical values (2 and 3) indicating that the measured data are verified and of good quality [36]. The inhibition efficiencies $\% \text{IE}_{\text{EFM}}$ increase by increasing the studied inhibitor concentrations and was calculated as follows:

$$\% \text{IE}_{\text{EFM}} = [(1 - i_{\text{corr}}/i_{\text{corr}})] \times 100 \quad (4)$$

Where i_{ocorr} and i_{corr} are corrosion current densities in the absence and presence of inhibitor, respectively. The inhibition sufficiency obtained from this method is in the order: Compound(III) > Compound(II) > Compound(I).

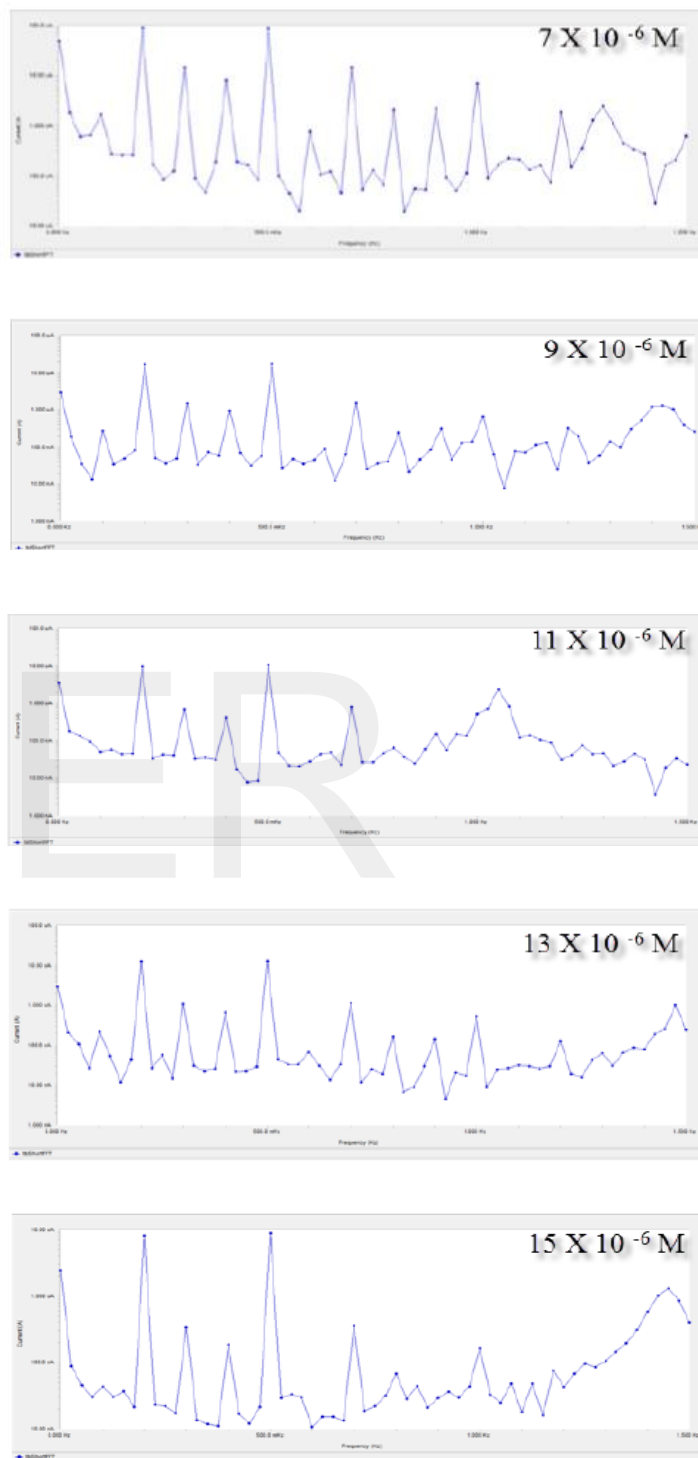
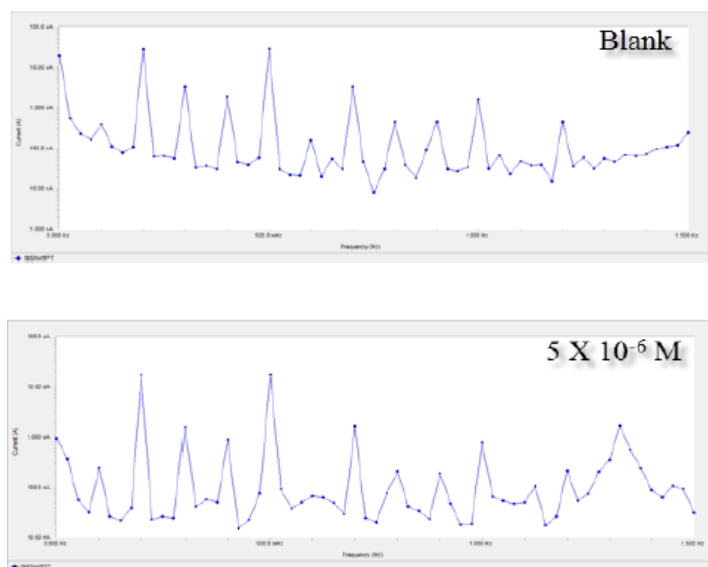


Fig. 6: EFM Spectra for Low C-steel Type (A) in 2M HCl in the Absence and Presence of Different Concentrations of Compound (I) at 25°C.

TABLE 7

ELECTROCHEMICAL KINETIC PARAMETERS OBTAINED BY EFM TECHNIQUE FOR LOW C-STEEL TYPE (A) IN THE ABSENCE AND PRESENCE OF VARIOUS CONCENTRATIONS OF INHIBITORS IN 2 HCL AT 25 °C.

Compound	Conc.,M	i_{corr} μAcm^{-2}	B_a $mVdec^{-1}$	B_c $mVdec^{-1}$	CF-2	CF-3	CR mpy	θ	%IE
	Blank	49.38	80.64	194.7	1.907	2.163	22.56	-	-
(I)	5×10^{-6}	31.64	88.90	180.7	1.895	3.405	14.46	0.359	35.9
	7×10^{-6}	30.5	68.4	219	1.93	2.810	14.07	0.382	38.2
	9×10^{-6}	25.46	76.7	135	1.937	2.905	11.63	0.484	48.4
	11×10^{-6}	24.01	115.5	242.2	1.558	2.880	10.97	0.514	51.4
	13×10^{-6}	22.48	87.63	167.6	1.88	2.040	10.18	0.545	54.5
	15×10^{-6}	21.92	138.2	211.7	1.994	2.226	10.02	0.556	55.6
(II)	5×10^{-6}	19.72	90.63	191.2	1.898	2.007	9.012	0.600	60.0
	7×10^{-6}	18.45	112.7	189.1	1.966	1.891	8.432	0.626	62.6
	9×10^{-6}	18.27	80.63	133	1.853	2.291	8.346	0.630	63.0
	11×10^{-6}	18	109.7	180.7	2.003	2.404	8.225	0.635	63.5
	13×10^{-6}	17.74	112.3	212.5	1.894	3.907	8.108	0.640	64.0
	15×10^{-6}	16.11	172.2	272.6	1.507	2.802	7.363	0.674	67.4
(III)	5×10^{-6}	15.78	116.5	236.6	1.920	9.921	7.209	0.680	68.0
	7×10^{-6}	14.83	93.07	131.4	2.196	1.501	6.775	0.699	69.9
	9×10^{-6}	14.53	90.94	134.3	4.993	1.984	6.64	0.706	70.6
	11×10^{-6}	13.82	85.48	131.8	1.620	2.544	6.22	0.720	72.1
	13×10^{-6}	13.50	90.68	149.1	1.699	2.529	6.168	0.727	72.7
	15×10^{-6}	12.62	99.56	150.5	1.975	2.637	5.767	0.744	74.4

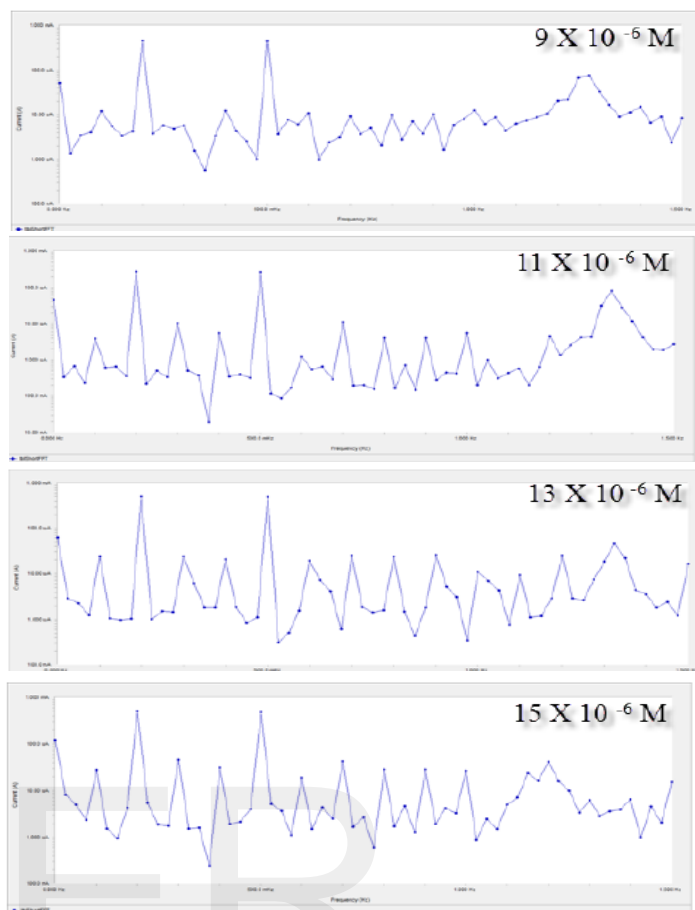
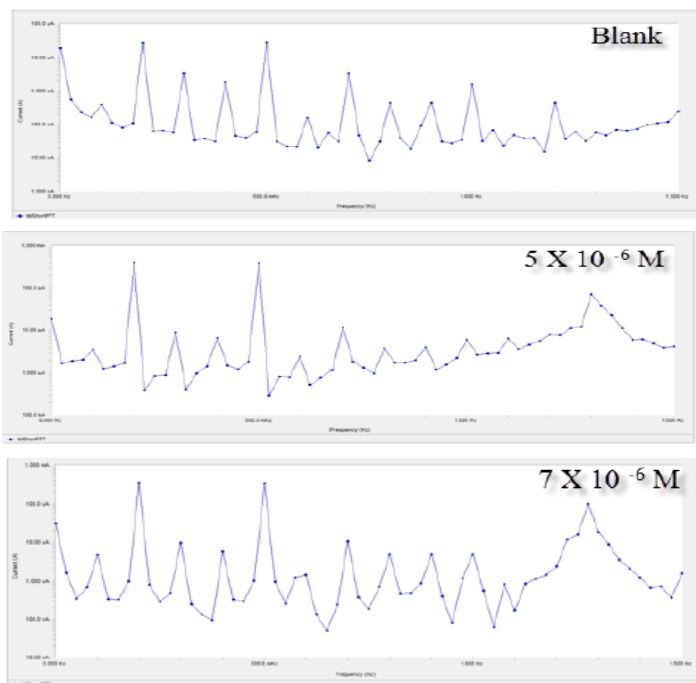


Fig. 7: EFM Spectra for Low C-steel Type (B) in 2M HCl in the Absence and Presence of Different Concentrations of Compound (I) at 25°C.

TABLE 8

ELECTROCHEMICAL KINETIC PARAMETERS OBTAINED BY EFM TECHNIQUE FOR LOW C-STEEL TYPE (B) IN THE ABSENCE AND PRESENCE OF VARIOUS CONCENTRATIONS OF INHIBITORS IN 2 HCL AT 25 °C.

Compound	Conc.,M	i_{corr} μAcm^{-2}	β_c $mVdec^{-1}$	β_a $mVdec^{-1}$	CF-2	CF-3	CR mpy	θ	%IE
	Blank	909.3	121.8	161.1	1.97	3.09	414.11	-	-
(I)	5×10^{-6}	548.9	97.4	115.4	1.93	2.27	296.5	0.397	39.7
	7×10^{-6}	537.6	94.4	114.2	1.88	2.85	245.7	0.408	40.8
	9×10^{-6}	444.9	65.4	70.11	2.06	3.03	217.0	0.511	51.1
	11×10^{-6}	401.1	85.3	107.4	1.93	2.92	183.3	0.558	55.8
	13×10^{-6}	400.4	84.4	56.8	1.95	2.93	183	0.559	55.9
	15×10^{-6}	359.5	41.8	43.3	1.89	3.01	134.3	0.604	60.4
(II)	5×10^{-6}	294.0	78.8	89.9	2.04	2.89	133.3	0.676	67.6
	7×10^{-6}	291.7	33.1	33.8	1.86	3.02	129.5	0.679	67.9
	9×10^{-6}	283.3	26.9	28.1	1.92	3.07	113.6	0.688	68.8
	11×10^{-6}	282.2	32.9	33.7	2.02	3.01	128.9	0.689	68.9
	13×10^{-6}	273.3	30.9	32.6	2.01	2.89	124.9	0.699	69.9
	15×10^{-6}	248.6	54.5	60.4	1.89	2.95	105.9	0.726	72.6
(III)	5×10^{-6}	231.8	38.5	39.2	2.06	2.97	81.8	0.745	74.5
	7×10^{-6}	179.0	51.5	53.3	1.89	2.93	80.0	0.803	80.3
	9×10^{-6}	175.3	48.5	51.6	1.88	2.89	77.8	0.807	80.7
	11×10^{-6}	170.3	45.7	48.4	2.03	3.09	52.6	0.812	81.2
	13×10^{-6}	115.2	43.6	50.7	2.01	3.07	45.0	0.873	87.3
	15×10^{-6}	50.49	74.1	77.2	1.95	2.99	23.0	0.944	94.4



3.4. Quantum Chemical Calculations

Theoretical calculations were performed for only the neutral forms, in order to give further insight into the experimental results. Values of quantum chemical indices such as energies of LUMO and HOMO (E_{HOMO} and E_{LUMO}), the formation heat ΔH_f and energy gap ΔE , are calculated by semi-empirical AM1, MNDO and PM3 methods has been given in Table (9). The reactive ability of the inhibitor is related to E_{HOMO} , E_{LUMO} [37]. Higher E_{HOMO} of the adsorbent leads to higher electron donating ability [38]. Low E_{LUMO} indicates that the acceptor accepts electrons easily. The calculated quantum chemical indices (E_{HOMO} , E_{LUMO} , μ) of investigated compounds are shown in Table (9). The difference $\Delta E = E_{\text{LUMO}} - E_{\text{HOMO}}$ is the energy required to move an electron from HOMO to LUMO. Low ΔE facilitates adsorption of the molecule and thus will cause higher inhibition efficiency. The bond gap energy ΔE increases from (III to I). This fact explains the decreasing inhibition efficiency in this order (III > II > I), as shown in Table (9) and Fig. (8) show the optimized structures of the three investigated compounds. So, the calculated energy gaps show reasonably good correlation with the efficiency of corrosion inhibition. Table (9) also indicates that compound (III) possesses the lowest total energy that means that compound (III) adsorption occurs easily and is favored by the highest softness. The HOMO and LUMO electronic density distributions of these molecules were plotted in Fig. (8). For the HOMO of the studied compounds that the benzene ring, N-atoms and O-atom have a large electron density. The data presented in Table (9) show that the calculated dipole moment decrease from (III > II > I).

TABLE 9

THE CALCULATED QUANTUM CHEMICAL PROPERTIES FOR 3-CARBOHYDRAZIDE DERIVATIVES.

	Compound (I)	Compound (II)	Compound (III)
$-E_{\text{HOMO}}$ (eV)	8.538	8.501	8.248
$-E_{\text{LUMO}}$ (eV)	0.192	0.868	0.898
ΔE (eV)	8.346	7.633	7.350
I_f (eV)	4.173	3.817	3.675
σ (eV ⁻¹)	0.240	0.262	0.272
$-P_i$ (eV)	4.365	4.685	4.573
(eV) χ	4.365	4.685	4.573
Dipole moment (Debye)	3.424	3.794	5.670

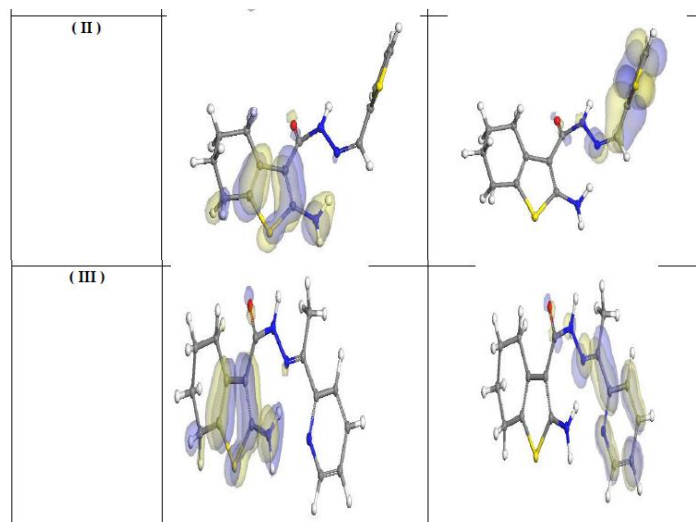
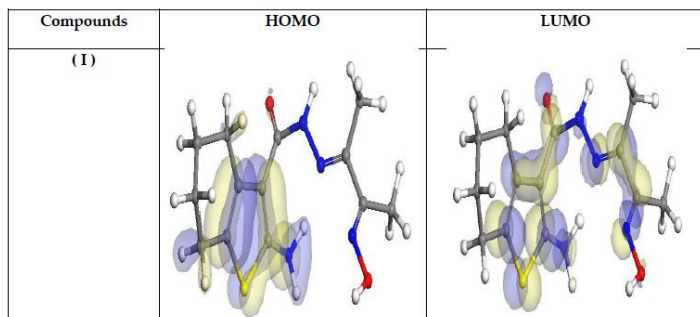


Fig 8.: Molecular Orbital Plots of 3-Carbohydrazide Derivatives.

3.5. Effect of Copper Addition on Corrosion Behavior of Low C-Steel

The use of low C-steel obtained by powder metallurgy (PM) has grown considerably in recent years [39]. A justification for the use of powder metallurgy low C-steel as a corrosion resistant material was presented as well as the potential advantages of preparing the alloy by surface cladding. This technique could overcome the problem of the high cost of the material and reduce the consumption of strategic rare elements. Moreover, PM techniques provide raw materials savings, dimensional accuracy and a good finishing that make machining unnecessary. PM cladding offers a cladding method with simple technological process. However, sintered low C-steel do have lower corrosion resistance than their corresponding cast or wrought equivalents [40, 41]. Interconnected porosity affects electrochemical behavior, increases reaction surface area, and promotes the formation of cells with local pH variation, hindering passivity. Consequently, the continued successful application of PM low C-steel will depend on process improvements to increase their corrosion resistance in aggressive media [42]. These improvements will include better control of sintering parameters, and some alloy modification through the addition of elements such as Cu. The aim of this study was to obtain low C-steel alloying with Cu by PM cladding and to investigate the corrosion performance of the alloy thus obtained. The distribution of Cu is more uniform. This is because the diffusion of Cu is easy at sintering temperature due to its low melting point. In addition, the density of Cu is greater than that of the low C-steel, which obviously becomes more important as increases. Cu alloying increased the passivation tendency of low C-steel clad specimen when using 4% concentration, while for higher concentrations the passivation extent became lower, although all materials were still passive. When the added Cu content was lower than 4%, they existed in the austenitic matrix in the solid solution. The solutioned Cu can enhance the cathodic reaction (hydrogen evolution) depolarization process, increasing the tendency to passivation [43-45]. When the addition of Cu content is over 4%, some free Cu would exist in the matrix. Because the free Cu intrinsically has lower corrosion resistance than that of the low C-steel, therefore, more than 4% Cu



addition decreased the corrosion resistance in the 2M HCl solution. The corrosion resistance of alloyed low C-steel surface layer with

Cu was better than that of C-steel surface layer in the 2M HCl solution [46].

3.6. Chemical Structure of the Inhibitors and Corrosion Inhibition

Inhibition of the corrosion of different types of low C-steel in 2 M HCl solution by some 3-carbohydrazide derivatives is determined by potentiodynamic anodic polarization measurements and other methods, it was found that the inhibition efficiency depends on concentration, nature of metal, the mode of adsorption of the inhibitors and surface conditions. The observed corrosion data in presence of these inhibitors, namely:

- The decrease of corrosion rate and corrosion current with increase in concentration of the inhibitor.
- The shift in Tafel lines to higher and lowers potential regions.
- The inhibition efficiency was shown to depend on the number of adsorption active centers in the molecule and their charge density.

The corrosion inhibition is due to adsorption of the inhibitors at the electrode/solution interface, the extent of adsorption of an inhibitor depends on the nature of the metal, the mode of adsorption of the inhibitor and the surface conditions. Adsorption on different types of low C-steel surface is assumed to take place mainly through the active centers attached to the inhibitor and would depend on their charge density. Transfer of lone pairs of electrons on the nitrogen atoms to the different types of low C-steel surface to form a coordinate type of linkage is favored by the presence of a vacant orbital in iron atom of low energy. Polar character of substituents in the changing part of the inhibitor molecule seems to have a prominent effect on the electron charge density of the molecule. It was concluded that the mode of adsorption depends on the affinity of the metal towards the π -electron clouds of the ring system. Metals such as Cu and Fe, which have a greater affinity towards aromatic moieties, were found to adsorb benzene rings in a flat orientation. The order of decreasing the inhibition efficiency of the investigated compounds in the corrosive solution was as follow: Compound(III) > Compound(II) > Compound(I).

The adsorption of inhibitor depends on its concentration. As shown in Fig. (9), at adsorption density less than a monolayer (Fig. 9a), most of the nucleation sites are still possibly exposed to HCl, since inhibitor adsorbs less likely on them. When the adsorption density reaches monolayer adsorption (Fig. 9b), some of the nucleation sites begin to be covered by inhibitor molecules. At maximum adsorption density (Fig. 9c), the inhibitor molecules cover the whole surface, including the nucleation sites, and then complete inhibition occurs.

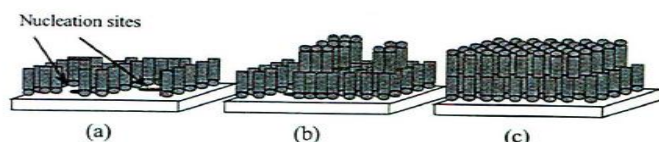


Fig. 9: Adsorption Schemes for 3-Carbohydrazide Derivatives as Inhibitors at: a) Low Concentration, on Low C-steel Surface, (b) Intermediate Concentration, on Low C-steel Surface, (c) High Concentration on Low C-steel Surface.

In general, two modes of adsorption are considered on the metal surface in acid media. In the first mode, the natural molecules may be adsorbed on the surface of low carbon steel through the chemisorption mechanism, involving the displacement of water molecules from the low C-steel surface and the sharing electrons between the hetero-atoms and iron the inhibitor molecules can also adsorb on the low carbon steel surface on the basis of donor- acceptor interactions between π -electrons of the aromatic ring and vacant d-orbitals of surface iron atoms in the second mode, since it is well known that the steel surface bears positive charge in acid solution [47, 48], so it is difficult for the protonated molecules to approach the positively charged low C-steel surface due to the electrostatic repulsion. Since chloride ions have a smaller degree of hydration, thus they could bring excess negative charges in the vicinity of the interface and favor more adsorption of the positively charged inhibitor molecules, the protonated 3-carbohydrazide derivatives adsorb through electrostatic interactions between the positively charged molecule and the negatively charged metal surface.

Compound (3) exhibits excellent inhibition power due to: (i) its larger molecular size (341.41) that may facilitate better surface coverage, and (ii) the presence electron releasing groups (4N, 1O and 1S atoms) which enhance the delocalized π -electrons on the active centers of the compound. Compound (2) comes after compound (3) in inhibition efficiency because it has lesser molecular size (305.42) and 1O, 2S and 3N atoms as active centers. Compound (1) has the lowest inhibition efficiency, this is due to it has the lowest molecular size (294.37).

4. CONCLUSIONS

The tested 3-carbohydrazide derivatives establish a very good inhibition for different types of low C-steel corrosion in HCl solution.

3-carbohydrazide derivatives inhibit different types of low C-steel corrosion by adsorption on its surface and act better than the passive oxide film.

The inhibition efficiency is in accordance to the order: (III) > (II) > (I).

Double layer capacitances decrease with respect to blank solution when the inhibitor added. This fact may explain by adsorption of the inhibitor molecule on the different types of low C-steel surface.

The values of inhibition efficiencies obtained from the different independent techniques showed the validity of the obtained results.

Quantum chemistry calculation results showed that the heteroatoms of N and S are the active sites of the 3-carbohydrazide derivatives. It can adsorb on Fe surface firmly by donating electrons to Fe atoms and accepting electrons from 3d orbitals of Fe atoms.

The corrosion resistance of alloyed low C-steel surface layer with 1% Cu was better than alloyed low C-steel surface layer with 0.5 % Cu.

REFERENCES

- [1] M. H. Wahdan, A. A. Hermas, M. S. Morad, *Mater. Chem. Phys.* 76 (2002) 111–118.
- [2] F. Bentiss, M. Lebrini, H. Vezin, M. Lagrennee, *Mater. Chem. Phys.* 87 (2004) 18–23.
- [3] X. Liu, P. C. Okafor, Y. G. Zheng, *Corros. Sci.* 51 (2009) 744–751.
- [4] G. E. Badr, *Corros. Sci.* 51 (2009) 2529–2536.
- [5] P. C. Okafor, Y. G. Zheng, *Corros. Sci.* 51 (2009) 850–859.
- [6] C. Kustu, K. C. Emregul, O. Atakol, *Corros. Sci.* 49 (2007) 2800–2814.
- [7] A. Ostovari, S. M. Hoseinie, M. Peikari, S. R. Shadizadeh, S. J. Hashemi, *Corros. Sci.* 51 (2009) 1935–1949.
- [8] M. J. Bahrami, S. M. A. Hosseini, P. Pilvar, *Corros. Sci.* 52 (2010) 2793–2803.
- [9] M. M. Solomon, S. A. Umoren, I. I. Udosoro, A. P. Udoh, *Corros. Sci.* 52 (2010) 1317–1325.
- [10] H. L. Wang, R. B. Liu, J. Xin, *Corros. Sci.* 46(2004) 2455–2466.
- [11] R. Solmaz, G. Kardas, B. Yazici, *Prot. Met.* 41 (2005) 581–585.
- [12] K. C. Emregul, R. Kurtaran, O. Atakol, *Corros. Sci.* 45 (2003) 2803–2817.
- [13] D. Chebabe, Z. A. Chikh, N. Hajjaji, A. Srhiri, F. Zucchi, *Corros. Sci.* 45 (2003) 309–320.
- [14] F. G. Liu, M. Du, J. Zhang, *Corros. Sci.* 51 (2009) 102–109.
- [15] A. Y. Musa, A. A. H. Kadhum, A. B. Mohamad, M. S. Takriff, *Corros. Sci.* 52 (2010) 3331–3340.
- [16] K. F. Khaled, M. A. Amin, *Corros. Sci.* 51 (2009) 1964–1975.
- [17] M. A. Quraishi, M. Z. A. Rafiquee, *J. Appl. Electrochem.* 37 (2007) 1153–1162.
- [18] X. Y. Zhang, F. P. Wang, Y. F. He, *Corros. Sci.* 43 (2001) 1417–1431.
- [19] M. Knag, K. Bilkova, E. Gulbrandsen, P. Carlsen, J. Sjoblom, *Corros. Sci.* 48 (2006) 2592–2613.
- [20] L. Wang, G. J. Yin, J. G. Yin, *Corros. Sci.* 43 (2001) 1197–1202.
- [21] P. C. Okafor, X. Liu, Y. G. Zheng, *Corros. Sci.* 51 (2009) 761–768.
- [22] J. Zhang, J. X. Liu, W. Z. Yu, Y. G. Yan, L. You, L. F. Liu, *Corros. Sci.* 52 (2010) 2059–2065.
- [23] L. M. Rodriguez-Valdez, W. Villamizar, M. Casales, *Corros. Sci.* 48 (2006) 4053–4064.
- [24] T. Arslan, F. Kandemirli, E. E. Ebenso, L. Love, H. Alemu, *Corros. Sci.* 51(2009) 35–47.
- [25] N. Khalil, *Electrochim. Acta* 48 (2003) 2638–2640.
- [26] M. E. Matheus, L. F. Oliveira, A. C. Freitas, A. M. Carvalho and A. J. Barreiro, *J. Med. Biol.* 24 (1991) 1219–1222.
- [27] R. W. Bosch, J. Hubrecht, W. F. Bogaerts, B. C. Syrett, *Corrosion* 57 (2001) 60.
- [28] S. S. Abdel-Rehim, K. F. Khaled, N. S. Abd-Elshafi, *Electrochim. Acta* 51 (2006) 3269.
- [29] E. Stupnisek-Lisac, A. Gazivoda and M. Madzarac, *J. Electrochim. Acta*, 47 (2002) 4189.
- [30] G. N. Mu, X. H. L. and Q. Quand, *J. Zhou, Corros. Sci.*, 48 (2006) 445.
- [31] I. Sekine, M. Sabongi, H. Hagiuda, T. Oshibe, M. Yuasa, T. Imahc, Y. Shibata, and T. Wake; *J. Electrochem. Soc.*; 139 (1992) 3167.
- [32] L. Larabi, O. Benali, S. M. Mekelleche and Y. Harek, *Appl. Surf. Sci.*, 253 (2006) 1371.
- [33] M. Lagrennee, B. Memari, B. Bouanis, M. Traisnel and F. Bentiss, *Corros. Sci.*, 44 (2002) 573.
- [34] G. A. Caignman, S. K. Metcalf, E. M. Holt, *J. Chem. Cryst.* 30 (2000) 415.
- [35] D. C. Silverman and J. E. Carrico, *National Association of Corrosion Engineers*, 44 (1988), 280.
- [36] R. A., Prabhu, T. V., Venkatesha, A. V., Shanbhag, G. M., Kulkarni, R. G., Kalkhambkar, *Corros. Sci.*, 50 (2008) 3356.
- [37] C. Lee, W. Yang and R. G. Parr, *Phys. Rev. B*, 37 (1988) 785.
- [38] R. M. Issa, M. K. Awad and F. M. Atlam, *Appl. Surf. Sci.*, 255 (2008) 2433.
- [39] W. Chen, Y. Wu and J. Shen, *Power Metall.*, 44 (2001) 309.
- [40] O. W. Reen and G. O. Hughes, *Precis. Met.*, (1977) 38.
- [41] R. Gold, *Precis. Met.*, (1982) 31.
- [42] W. E. Jones, *Power Metall.*, 2 (1981) 101.
- [43] J. H. Reinshagen and R. P. Mason, *Advances in Powder Metall.*, 5 (1992) 385.
- [44] D. Itzhak and P. Peled, *Corros. Sci.*, 26 (1986) 49.
- [45] L. Fedrizzi, A. Molinari, F. Deflorian, A. Tiziani and P. L. Bonora, *Proc. Int. Powder Metallurgy, Conf. And Exhibition, London, UK, July., 2 (1990) 319.*
- [46] F. Deflorian, L. Ciaghi and J. Kazior, *Werkstoffe und Korrosion*, 43 (1992) 447.
- [47] G. N. Mu, T. P. Zhao, M. liu and T. GU, *Corrosion* 52 (1996) 853.
- [48] A. K. Singh and M. A. Quraishi, *corros, Sci.*, 52 (2010) 1529.